

DOI: 10.1002/cctc.201300865

# A NiPdB-PEG(800) Amorphous Alloy Catalyst for the Chemoselective Hydrogenation of Electron-Deficient Aromatic Substrates

Guoyi Bai,\* Zhen Zhao, Huixian Dong, Libo Niu, Yalong Wang, and Qingzhi Chen<sup>[a]</sup>

A new Pd and polyethylene glycol 800 [PEG(800)]-modified NiB [NiPdB-PEG(800)] amorphous alloy catalyst was prepared, which demonstrated excellent activities, similar to those of noble metal catalysts, in the chemoselective hydrogenation of a series of electron-deficient aromatic substrates in water. The addition of small amounts of Pd to NiB markedly improved its activity. The Pd not only benefits the dispersion of active species but also contributes to the activity of the catalyst. The accompanying agglomeration can be inhibited with the further

addition of PEG(800), which results in the largest surface area, the smallest particle size, and the greatest number of active species, resulting in optimum H<sub>2</sub>-chemisorption and accounting for its highest activity. The key factors determining the main reaction products depend not only on the structures of the substrates but also on the character of the solvents. Water is found to be the most effective solvent for most of the substrates.

## Introduction

Cyclohexane and its derivatives are important intermediates in industry; in particular, cyclohexanol and cyclohexanone are key intermediates for the manufacture of nylon 66.<sup>[1]</sup> The preparation of cyclohexane derivatives through the catalytic hydrogenation of aromatic precursors has attracted much attention in recent years,<sup>[2]</sup> both in the laboratory and in industry, owing to the green nature of this process, the ready availability of suitable feedstocks, and the directness of the approach. Noble metals such as Pt, Pd, and Rh have been studied extensively for these transformations.<sup>[3]</sup> For example, Hubert et al. have obtained good results under mild experimental conditions in the catalytic hydrogenation of benzene derivatives over Rh-based nanocatalysts in water.<sup>[4]</sup> Taniya et al. have investigated Sn-modified SiO<sub>2</sub>-coated Pt catalysts for the chemoselective hydrogenation of crotonaldehyde and found that the role of the Sn promoter was to activate the aldehyde group of crotonaldehyde.<sup>[5]</sup> Snelders et al. have achieved chemoselectivities exceeding 90% in the hydrogenation of phenylacetone to cyclohexylacetone over Rh-based catalysts poisoned by phosphine ligands.<sup>[6]</sup> Unfortunately, the application of such catalysts in industry has been limited owing to the high price of noble metals. Meanwhile, reports of related studies using non-noble metal catalysts are scarce and such catalysts can achieve good results only under forcing reaction conditions.<sup>[7]</sup>

Amorphous alloys have attracted much attention owing to their interesting intrinsic properties such as short-range order, long-range disorder, and high dispersion, and so they have been widely used in catalytic hydrogenation.<sup>[8]</sup> Generally, amorphous alloys, especially NiB amorphous alloys, are prepared through the reduction of transition-metal salt solutions with potassium borohydride or sodium hypophosphite, which demonstrate excellent catalytic performance in the hydrogenation of alkenes and carbonyl compounds. The addition of metals,<sup>[9]</sup> complexing species,<sup>[10]</sup> and polymers<sup>[11]</sup> as well as the application of ultrasound<sup>[12]</sup> during the catalyst preparation process can play a key role in improving the activity of amorphous alloy catalysts. For example, Chen and Sasirekha have found that appropriate proportions of Fe in a NiB amorphous alloy catalyst could suppress the growth of crystalline NiFeB and the Ni possessed more d-band electrons and higher electron density than the undoped NiB amorphous alloy, which leads to higher activity in the hydrogenation of *p*-chloronitrobenzene.<sup>[13]</sup> However, there are few reports on the hydrogenation of aromatic substrates over amorphous alloy catalysts and such reports are mainly limited to electron-rich aromatic substrates, such as phenol,<sup>[14]</sup> owing to the relatively lower catalytic activity of NiB amorphous alloys compared with noble metal catalysts. To our knowledge, no detailed studies on the hydrogenation of electron-deficient aromatic substrates over amorphous alloy catalysts have been reported.

In the continuation of our previous work,<sup>[15]</sup> we report herein our recent research into the hydrogenation of aromatic carboxylic acids and their derivatives over amorphous alloy catalysts and the selective hydrogenation of ethyl benzoate to ethyl cyclohexanecarboxylate was chosen as a model system. Considering the low activity of the pure NiB amorphous alloy catalyst, different modifications were surveyed to improve its

[a] Prof. G. Bai, Z. Zhao, H. Dong, L. Niu, Y. Wang, Q. Chen  
Key Laboratory of Chemical Biology of Hebei Province  
College of Chemistry and Environmental Science  
Hebei University  
Baoding, Hebei 071002 (P.R.China)  
Fax: (+86) 312-5937102  
E-mail: baiguoyi@hotmail.com

 Supporting information for this article is available on the WWW under <http://dx.doi.org/10.1002/cctc.201300865>.

activity. A Pd and polyethylene glycol 800 [PEG(800)]-modified NiB [NiPdB-PEG(800)] amorphous alloy catalyst demonstrated excellent catalytic performance, similar to that of noble metal catalysts, in this reaction. The effects of the amount of Pd added and the solvent were studied. Finally, to expand the scope of this protocol, we also investigated the hydrogenation of other aromatic carboxylic acids and their derivatives over NiPdB-PEG(800) under optimal conditions and efficient and selective conversions were observed. The result of these studies is the development of a new catalytic system, which demonstrates efficiency and chemoselectivity similar to those of noble metal-based catalysts but requires significantly reduced levels of Pd for use in water.

## Results and Discussion

### Hydrogenation of ethyl benzoate

Owing to the reluctance of electron-deficient aromatic substrates to undergo hydrogenation, the undoped NiB amorphous alloy demonstrated low activity in the hydrogenation of ethyl benzoate to ethyl cyclohexanecarboxylate. Considering the benefit of metal modification on amorphous alloys, a series of metal-doped NiB amorphous alloys were prepared and tested in this reaction, and the results are listed in Table 1.

Catalyst	Conversion [%]	Selectivity [%]	Yield [%]
NiB	15.2	98.2	14.9
NiCoB <sup>[b]</sup>	40.5	97.7	39.6
NiFeB <sup>[b]</sup>	31.6	97.1	30.7
NiLaB <sup>[b]</sup>	49.7	90.3	44.9
NiZrB <sup>[b]</sup>	51.3	93.9	48.2
NiPdB <sup>[b]</sup>	70.9	95.1	67.4
PdB <sup>[c]</sup>	36.2	88.5	31.9
NiB + PdB <sup>[d]</sup>	38.7	93.5	36.2

[a] Reaction conditions: Ethyl benzoate (5.0 g, 33 mmol), ethanol (70 mL), catalyst amount (0.2 g),  $P(\text{H}_2) = 5$  MPa, 400 rpm, 423 K, 5 h; [b] Molar ratio of Ni to other metals is 20:1; [c] The amount of PdB is 0.023 g; [d] The amount of NiB and PdB are 0.177 and 0.023 g, respectively.

As expected, all metal-doped NiB amorphous alloys demonstrated better catalytic performance than the undoped amorphous alloy mainly owing to their dispersive effect.<sup>[16]</sup> The addition of small amounts of Pd to the NiB amorphous alloy (molar ratio of Ni to Pd is 20:1) markedly increased the conversion of ethyl benzoate from 15.2 to 70.9%. Furthermore, NiPdB demonstrated much better catalytic performance than the physical mixture of NiB and PdB, with the same proportion of Ni and Pd as in NiPdB. The physical mixture of NiB and PdB demonstrated activity similar to that of PdB of the same weight (Table 1). Thus, we suggest that the small amount of Pd not only leads to fine dispersion of Ni species but also contributes to the high activity of NiPdB.

A conversion of ethyl benzoate of 70.9% and a selectivity toward ethyl cyclohexanecarboxylate of 95.1% are good results for a NiB amorphous alloy doped with such a small amount (0.2 mmol) of Pd, although it was still lower than that in standard noble metal catalysts. Considering the benefit of polymer modification in our previous studies,<sup>[15]</sup> a series of polymers were then used as modifiers for the NiPdB amorphous alloy catalyst to improve its activity, and the results are listed in Table 2. As expected, the addition of PEG improved

Catalyst <sup>[b]</sup>	Conversion [%]	Selectivity [%]	Yield [%]
NiPdB	70.9	95.1	67.4
NiPdB-PVP	40.4	98.3	39.7
NiPdB-PVA	48.0	98.9	47.5
NiPdB-PAA	7.5	99.6	7.5
NiPdB-PEG(400)	70.7	97.2	68.7
NiPdB-PEG(600)	80.7	95.1	76.7
NiPdB-PEG(800)	96.1	95.3	91.6
NiPdB-PEG(1000)	91.9	95.9	88.1
NiPdB-PEG(2000)	86.0	94.9	81.6
NiPdB-PEG(10 000)	84.9	95.8	81.3
NiB-PEG(800)	37.4	95.9	35.9
c-NiPdB-PEG(800) <sup>[c]</sup>	1.0	100.0	1.0
Pd/C <sup>[d]</sup>	78.5	98.6	77.4
Raney Ni	29.4	90.2	26.5

[a] Reaction conditions: Ethyl benzoate (5.0 g, 33 mmol), ethanol (70 mL), catalyst amount (0.2 g),  $P(\text{H}_2) = 5$  MPa, 400 rpm, 423 K, 5 h; [b] Molar ratio of Ni to Pd is 20:1; [c] Catalyst was crystallized at 973 K; [d] 0.5 g, 5 wt% Pd.

the activity of the NiPdB amorphous alloy catalyst, whereas polyvinyl alcohol (PVA)-, polyvinylpyrrolidone (PVP)-, and especially polyacrylic acid (PAA)-modified amorphous alloys revealed minimal activity. We ascribed this result largely to the solubility of the polymers. Considering that PVA, PVP, and PAA partly dissolved in the precursor mixtures to give slightly viscous solutions, we propose that the in situ prepared NiPdB particles would mainly adsorb onto the surface of the undissolved polymers, leading to a decrease in the activity of these modified amorphous alloy catalysts. In contrast, PEGs, especially low molecular mass PEGs, are soluble polymers and can prevent the agglomeration of the particles during the reduction process to attain more active Ni species. PEGs are also considered as reducing agents and stabilizers in the preparation of nanoparticles, as Harraz et al. have reported previously.<sup>[17]</sup> Furthermore, the conversion of ethyl benzoate first increased and then decreased with the increase in molecular mass of PEG used for the PEG-modified NiPdB amorphous alloys. Of all the PEG-modified NiPdB amorphous alloys, NiPdB-PEG(800) demonstrated the best conversion (96.1%), together with a high selectivity (95.3%) toward ethyl cyclohexanecarboxylate, which is ascribed to the appropriate molecular mass and good solubility of PEG(800). The activity of NiPdB-PEG(800) is higher than that of Pd/C and commercial Raney Ni under similar reaction conditions (Table 2), but lower than that of the Ru-based cata-

lyst.<sup>[18]</sup> Given that the conversion of ethyl benzoate over NiB-PEG(800) was only 37.4%, Pd is believed to have a greater effect on the high activity of NiPdB-PEG(800) than PEG(800).

Further studies showed that the activities of NiPdB-PEG(800) increased with the increase in the amount of Pd in NiPdB-PEG(800). The conversion of ethyl benzoate increased from 52.1 to 98.3% with the decrease in the molar ratio of Ni to Pd from 40:1 to 10:1. Thus, the addition of a small amount of Pd and PEG(800) can remarkably improve the activity of the NiB amorphous alloy owing to the synergistic effect between Pd and PEG(800), and NiPdB-PEG(800) was finally chosen as the catalyst of choice for the chemoselective hydrogenation of ethyl benzoate to produce ethyl cyclohexanecarboxylate.

The reaction conditions were also preliminarily optimized (see the Supporting Information). It was proven that there was no mass or heat transfer limitation while the stirring rate was 400 rpm or more.<sup>[19]</sup> The conversion of ethyl benzoate increased with the increase in hydrogen pressure and reaction temperature. Eventually, 5 MPa hydrogen pressure, 423 K, and 400 rpm is considered an appropriate reaction condition for this hydrogenation process.

### Catalyst characterization

The compositions, Brunauer–Emmett–Teller (BET) surface areas, H<sub>2</sub>-chemisorptions, average particle sizes, and turnover frequencies (TOFs) of NiB, NiPdB, and NiPdB-PEG(800) were measured, and selected results are summarized in Table 3. From the inductively coupled plasma (ICP) analysis, it was found that NiPdB contained the same ratio of B in the bulk as NiB and the contents of both Pd and B increased slightly with the further addition of PEG(800). As the noble metal Pd has a greater capacity for adsorbing and releasing hydrogen than the transition-metal Ni,<sup>[20]</sup> more Pd helps to improve the catalyst's activity in hydrogenation. Although the BET surface area and H<sub>2</sub>-chemisorption of NiB increased to some extent with the addition of Pd, both increased markedly with the further addition of PEG(800). The BET surface area increased from 14 to 27 m<sup>2</sup>g<sup>-1</sup> and H<sub>2</sub>-chemisorption increased from 0.33 to 0.61 cm<sup>3</sup>g<sup>-1</sup> owing to the dispersive effect and reductive character of PEG(800). In contrast, the average particle size decreased from 9.5 to 9.3 and 8.7 nm with the addition of Pd and PEG(800), respectively. Of the catalysts studied, NiPdB-PEG(800) has the largest surface area, the greatest number of active species, and the smallest particle size, probably owing to the synergistic effect between Pd and PEG(800), which ac-

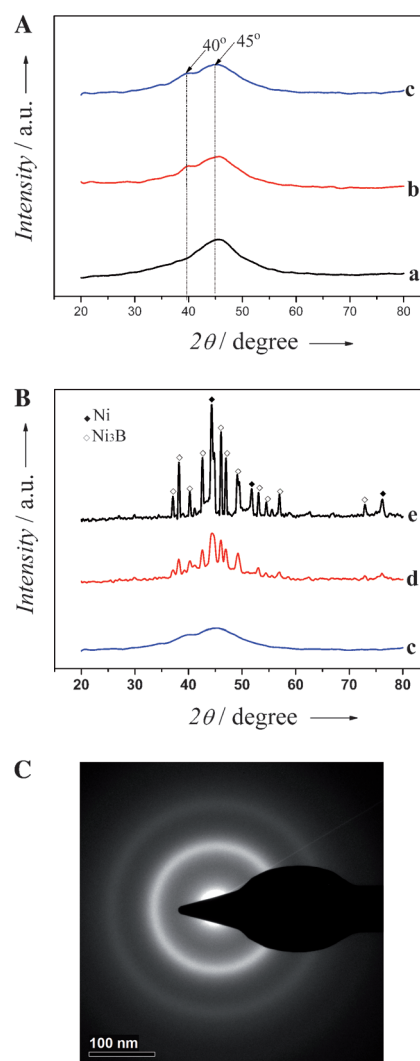


**Figure 1.** XRD patterns of the amorphous alloy catalysts. A: a) NiB, b) NiPdB, c) NiPdB-PEG(800). B: c) NiPdB-PEG(800), d) NiPdB-PEG(800) treated at 573 K, e) NiPdB-PEG(800) treated at 973 K. C: SAED image of the NiPdB-PEG(800).

counts for its highest activity in the hydrogenation of ethyl benzoate and is in agreement with the TOF values of these amorphous alloy catalysts.

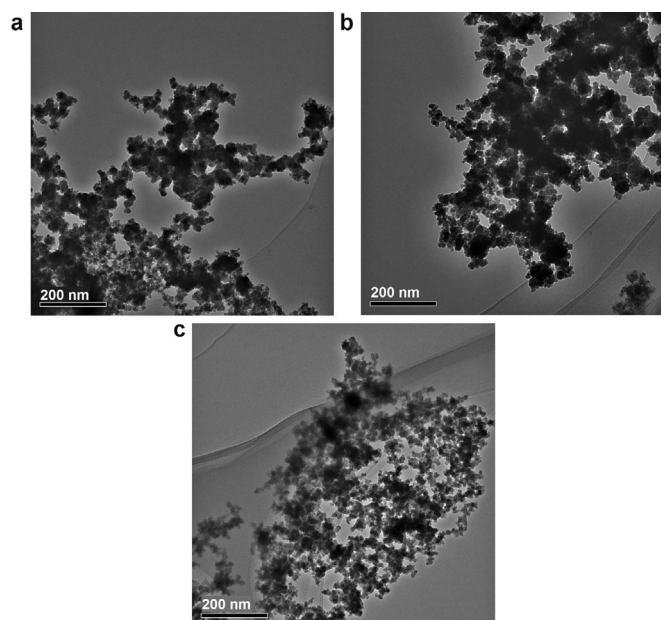
The X-ray diffraction (XRD) patterns of NiB, NiPdB, and NiPdB-PEG(800) are shown in Figure 1. A broad peak at  $2\theta = 45^\circ$  was observed for each freshly prepared catalyst, which is indicative of a typical NiB amorphous structure<sup>[15]</sup> and can also be confirmed by a successive diffraction halo in the selected area electron diffraction (SAED) image (Figure 1C).<sup>[22]</sup> This finding indicates that the addition of Pd and PEG(800) had not changed the amorphous structure of these NiB catalysts. In contrast, increasing the treatment temperature of NiPdB-PEG(800) to 573 K in a N<sub>2</sub> atmosphere led to the appearance of weak characteristic peaks corresponding to

Table 3. Selected physicochemical properties of the amorphous alloy catalysts.					
Catalyst	Composition (atomic ratio) <sup>[a]</sup>	Surface area [m <sup>2</sup> g <sup>-1</sup> ]	H <sub>2</sub> -chemisorption [cm <sup>3</sup> g <sup>-1</sup> ]	Particle size <sup>[b]</sup> [nm]	TOF <sup>[c]</sup> [10 <sup>2</sup> h <sup>-1</sup> ]
NiB	Ni <sub>1.00</sub> B <sub>0.38</sub>	11	0.24	9.5	2.34
NiPdB	Ni <sub>1.00</sub> Pd <sub>0.04</sub> B <sub>0.38</sub>	14	0.33	9.3	5.69
NiPdB-PEG(800)	Ni <sub>1.00</sub> Pd <sub>0.05</sub> B <sub>0.41</sub>	27	0.61	8.7	6.26

[a] Based on ICP results; [b] Estimated from TEM results; [c] TOF values were calculated on the basis of the number of moles of ethyl benzoate converted per mole of active metal per hour, according to Ref. [21].

crystalline Ni and Ni<sub>3</sub>B.<sup>[23]</sup> With the increase to 973 K, these peaks became sharp, together with the disappearance of the characteristic peak of the amorphous alloy (Figure 1B), which demonstrates the transformation of nanoparticles from an amorphous state to a crystalline state. Furthermore, the shoulder peak at  $2\theta \approx 40^\circ$  in the Pd-doped catalysts can be ascribed to the characteristic peak of PdB,<sup>[24]</sup> which can disperse and activate the amorphous Ni, giving the catalyst higher surface area and H<sub>2</sub>-chemisorption value. This peak disappeared after the high-temperature treatment, probably because the peaks corresponding to crystallized Pd were obscured by the characteristic peaks of Ni<sub>3</sub>B.<sup>[25]</sup> A comparative experiment established that NiPdB-PEG(800) that had crystallized at 973 K demonstrated no activity in the hydrogenation of ethyl benzoate (Table 2), which proved that the amorphous structure of NiPdB-PEG(800) was crucial to its high activity.

The surface morphology of the amorphous alloy catalysts was recorded by using transmission electron microscopy (TEM; Figure 2). It appears that each sample demonstrated approximately spherical morphology, consistent with other reported



**Figure 2.** TEM morphologies of the amorphous alloy catalysts: a) NiB, b) NiPdB, and c) NiPdB-PEG(800).

Ni-based amorphous alloy catalysts.<sup>[11]</sup> The particle distribution decreased from 6.1–14.8 to 6.0–12.8 nm upon addition of Pd, although some agglomeration still took place in NiPdB. The agglomeration may result in some coverage of active centers and consequently diminish the extent of H<sub>2</sub>-chemisorption. However, the effect of Pd addition appears to be advantageous on the catalyst's structure, which results in a larger surface area and higher H<sub>2</sub>-chemisorption as compared with those of NiB. Moreover, this agglomeration phenomenon could be inhibited with the further addition of PEG(800). The particles in NiPdB-PEG(800) were well dispersed and the particle distribution decreased further to 7.1–10.7 nm, which resulted in the highest

surface area and H<sub>2</sub>-chemisorption of this catalyst. In contrast, no evidence for the existence of PEG(800) on the surface of NiPdB-PEG(800) could be found from the TEM investigation. Thus, we propose that most of the PEG(800) polymer has been removed during washing in the preparation process and its main role was to prevent agglomeration of the amorphous alloy particles in the reduction process, which resulted in more active Pd and Ni species; this observation is also reported in our previous work<sup>[15]</sup> and is in accordance with the ICP and H<sub>2</sub>-chemisorption results.

The temperature-programmed desorption of hydrogen (H<sub>2</sub>-TPD) profiles of the three samples are shown in Figure 3. NiB shows three peaks at approximately 447, 539, and 605 K, which indicate the presence of three adsorbing sites. In contrast, both NiPdB and NiPdB-PEG(800) show one strong peak at approximately 600 K, together with a small peak at approxi-

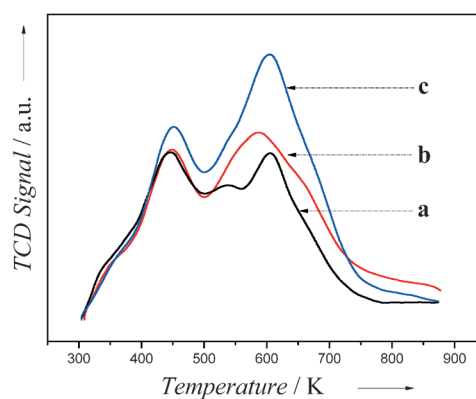


**Figure 3.** H<sub>2</sub>-TPD spectra of the amorphous alloy catalysts: a) NiB, b) NiPdB, and c) NiPdB-PEG(800). TCD = thermal conductivity detector.

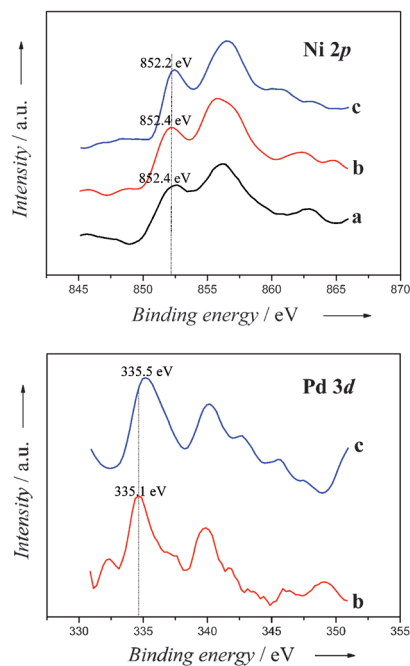


**Figure 4.** XPS spectra of Ni 2p and Pd 3d of the amorphous alloy catalysts: a) NiB, b) NiPdB, and c) NiPdB-PEG(800).

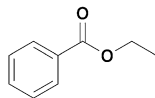
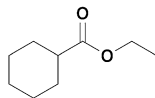
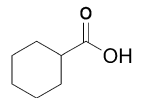
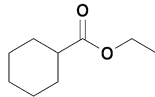
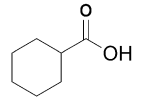
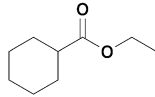
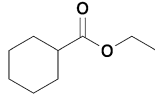
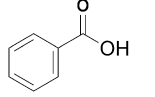
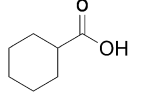
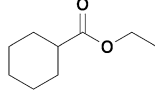
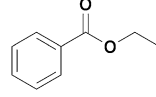
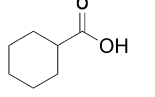
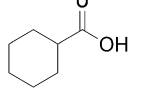
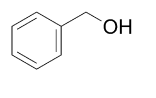
mately 450 K, and thus it can be concluded that active Ni species of the catalysts tend to become uniform in the presence of Pd.<sup>[26]</sup> Furthermore, the hydrogen desorption peaks of NiPdB-PEG(800) are much larger than those of the other two catalysts, especially the peaks at approximately 600 K, which indicate that the addition of PEG(800) could favor the dispersion of nanoparticles in the catalyst, resulting in the formation of more active centers, which is in agreement with the H<sub>2</sub>-chemisorption results. In combination with the experimental results, it reveals that the high-temperature hydrogen-absorbing sites are more beneficial to the hydrogenation of ethyl benzoate.

The X-ray photoelectron spectroscopy (XPS) spectra of Ni2p and Pd3d of the amorphous alloy catalysts are shown in Figure 4. The characteristic peaks of Ni2p centered at approximately 852 and 856 eV in all samples can be assigned to metallic and oxidized Ni, respectively. The characteristic peaks of Pd3d centered at approximately 335 eV confirm the presence of metallic Pd in the catalysts, which are active in hydrogenation.<sup>[27]</sup> Thus, metallic Ni is considered as active species of the catalysts<sup>[15]</sup> and the added Pd not only benefits the dispersion of active Ni species but also contributes to the activity of the catalysts.

#### Effects of solvent and substrate

To test the effect of the solvent, the hydrogenation of ethyl benzoate and benzoic acid was studied in various solvents over NiPdB-PEG(800) under the same reaction conditions (Table 4). The hydrogenation of ethyl benzoate proceeded faster with 100.0% conversion in water than in ethanol; however, the selectivity toward ethyl cyclohexanecarboxylate decreased and cyclohexanecarboxylic acid was detected as the major byproduct owing to the hydrolysis of the resulting ethyl cyclohexanecarboxylate or the successive hydrolysis and hydrogenation of ethyl benzoate in water. In contrast, in the case of dioxane, the extent of hydrogenation was limited but the selectivity was excellent and only the ring hydrogenated product was detected. However, in the case of *n*-hexane, the hydrogenation proceeded faster with 89.2% conversion but lower selectivity toward ethyl cyclohexanecarboxylate (97.1%) as

**Table 4.** Hydrogenation of ethyl benzoate and benzoic acid in different solvents over NiPdB-PEG(800).<sup>[a]</sup>

Substrate	Solvent	Conversion [%]	Selectivity [%]	
			Main product	Byproduct
	water	100.0		 22.4
	ethanol	96.1		 1.7
	dioxane	25.5		-
	<i>n</i> -hexane	89.2		-
	water	97.6		-
	ethanol	100.0		 46.8
	dioxane	49.2		-
	<i>n</i> -hexane	83.5		 26.6

[a] Reaction conditions: Substrate (33 mmol), solvent (70 mL), catalyst (0.2 g), P(H<sub>2</sub>) = 5 MPa, 400 rpm, 423 K, 5 h.

compared with dioxane, probably owing to the difference in polarity of these two aprotic solvents.

Furthermore, the hydrogenation of benzoic acid yielded different results in water and ethanol (Table 4). The hydrogenation of benzoic acid proceeded effectively in water with 97.6% conversion and 100.0% selectivity toward cyclohexanecarboxylic acid, which we ascribe to the solvating and orientating effect of water on the carboxylic group, as also described by Anderson et al.<sup>[28]</sup> The conversion of benzoic acid was 100.0% in ethanol; however, ethyl benzoate and ethyl cyclohexanecarboxylate were detected as the two main products owing to the concomitant esterification of benzoic acid with the subsequent hydrogenation of ethyl benzoate thus formed, but cyclohexanecarboxylic acid was not detectable in the reaction mixture. Thus, it would appear that the catalyst promotes esterification before the hydrogenation in ethanol. In the case of dioxane, the hydrogenation of benzoic acid showed moderate conversion (49.2%) but 100.0% selectivity toward cyclohexanecarboxylic acid, whereas in the case of *n*-hexane, the hydrogenation proceeded faster with 83.5% conversion but 73.4% selectivity. Thus, water is regarded as the best solvent in the hydrogenation of benzoic acid owing to the high selectivity

demonstrated by the catalyst in this solvent and the overall green nature of the system.

To determine whether the high activity of NiPdB-PEG(800) was specific to ethyl benzoate and benzoic acid, a number of other electron-deficient aromatic substrates were studied (Table 5). NiPdB-PEG(800) demonstrated excellent activities with all substrates with 100.0% conversion in most cases except benzoic acid (97.6% conversion) and phenyl acetic acid (95.4% conversion). However, the selectivities varied markedly, depending on the structures of the substrates. In the case of methyl benzoate, cyclohexanecarboxylic acid was the main product instead of methyl cyclohexanecarboxylate, as compared to the case of ethyl benzoate. This finding is consistent with the higher susceptibility of methyl esters to aqueous hydrolysis compared to ethyl esters.<sup>[29]</sup> For various aromatic carboxylic acids, increasing the length of the carbon chain did not decrease the excellent conversion and selectivity toward the ring hydrogenated products. However, in the case of cinnamic acid, the side-chain olefinic double bond was also hydrogenated in the main product obtained. The best result was obtained in the hydrogenation of benzamide with both 100.0% conversion and selectivity toward cyclohexane carboxamide over NiPdB-PEG(800), which eclipsed the reported re-

sults for Pd on carbon nanofibers (CNFs).<sup>[28]</sup> In contrast, the hydrogenation of acetophenone and benzophenone showed different reactivities. 1-Cyclohexylethanol was detected as the main product in the hydrogenation of acetophenone, which yielded cyclohexyl methyl ketone as the main byproduct; this finding indicates that NiPdB-PEG(800) was active for the hydrogenation of both the aromatic ring and the carbonyl group in acetophenone. In contrast, cyclohexylmethylbenzene was obtained as the main product in the hydrogenation of benzophenone arising from the successive hydrogenation of diphenylmethane, the main byproduct, which in turn was obtained from the direct hydrogenolysis of the carbonyl group of benzophenone.<sup>[30]</sup>

## Conclusions

The presence of small amounts of Pd in a NiB amorphous alloy can introduce larger surface area, smaller particle size, and higher H<sub>2</sub>-chemisorption, although some agglomeration still occurred, and this markedly increased the conversion of ethyl benzoate on hydrogenation. The accompanying agglomeration could be inhibited with the further addition of PEG(800), which decreases the coverage of Ni centers and results in the highest

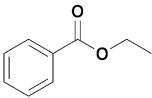
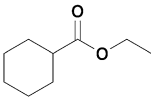
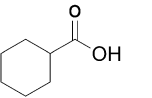
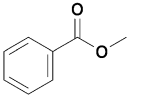
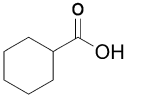
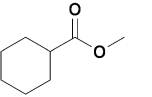
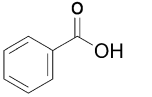
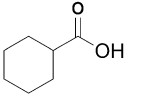
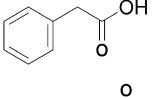
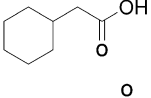
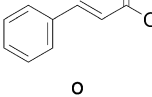
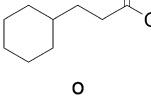
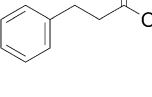
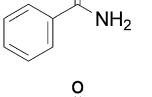
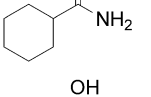
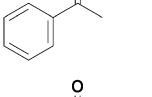
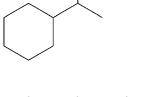
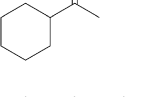
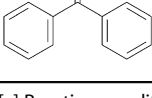
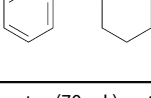
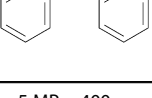
H<sub>2</sub>-chemisorption, the largest surface area, and the smallest particle size. NiPdB-PEG(800) demonstrated the highest activity in the chemoselective hydrogenation of ethyl benzoate comparable with noble metal catalysts; this finding indicates a synergistic effect between Pd and PEG(800), as confirmed by XPS and H<sub>2</sub>-TPD analyses. Furthermore, ethyl benzoate and benzoic acid showed different hydrogenation performance in different solvents. Finally, NiPdB-PEG(800) demonstrated excellent activities and selectivities in the hydrogenation of various electron-deficient aromatic substrates in water and is thus potentially applicable to large-scale productions. The significant reduction in the necessary amount of Pd is advantageous in this respect.

## Experimental Section

### Catalyst preparation

Unless otherwise stated, all chemicals were purchased from Baoding Huaxin Reagent and Apparatus Co. Ltd. and were used as received without further purification. Metal-

**Table 5.** Hydrogenation of different aromatic substrates over NiPdB-PEG(800) in water.<sup>[a]</sup>

Substrate	Conversion [%]	Main product	Selectivity [%]	
				Byproduct
	100.0		75.6	 22.4
	100.0		78.5	 21.5
	97.6		100.0	–
	95.4		100.0	–
	100.0		96.0	 4.0
	100.0		100.0	–
	100.0		63.6	 36.4
	100.0		50.9	 34.5

[a] Reaction conditions: Substrate (33 mmol), water (70 mL), catalyst (0.2 g), P(H<sub>2</sub>) = 5 MPa, 400 rpm, 423 K, 5 h.

and polymer-modified NiB amorphous alloys were prepared through chemical reduction. A typical method is as follows:  $\text{NiCl}_2 \cdot 6\text{H}_2\text{O}$  (0.94 g, 4.0 mmol) and the requisite amount of the soluble salts of Co, Fe, La, Zr, and Pd (X) in a molar ratio of  $\text{Ni}/\text{X} = 20:1$  were dissolved in distilled water (7.5 mL), and then the solution was treated with ultrasound for 5 min to ensure good mixing. Subsequently,  $\text{KBH}_4(\text{aq})$  (20 mmol, 17 mL, 1.3 M) containing NaOH (0.22 M) was added dropwise to the above solution with vigorous stirring while cooling in an ice bath until gas evolution ceased. The black precipitate thus obtained was washed with deoxygenated distilled water until the washings were pH 7. The catalyst was further washed 3 times with absolute ethanol to replace residual water and then stored in absolute ethanol. The catalysts so obtained are labeled NiXB. Upon the addition of the polymer (1.0 g) to the  $\text{NiCl}_2 \cdot 6\text{H}_2\text{O}$  and metal salt solutions during the preparation, the catalysts so obtained are labeled NiXB-*p*, in which *p* represented the nature of the polymer.

Pure NiB and PdB were also obtained through chemical reduction as reported previously.<sup>[21]</sup> The physical mixture of NiB and PdB was obtained by physically mixing the previously prepared NiB and PdB. Otherwise, the Pd/C catalyst was purchased from Tianjin Kermel Chemical Reagent Co. Ltd. Raney Ni was prepared through alkali leaching of the Ni–Al alloy by using the conventional method.<sup>[31]</sup>

### Catalyst characterization

Bulk compositions of the amorphous alloy catalysts were determined from ICP analysis on a Varian Vista MPX spectrometer. All samples were first treated with concentrated  $\text{HNO}_3/\text{H}_2\text{SO}_4$  solution (1:1 volume ratio) at RT, then diluted to the requisite concentration, and finally analyzed to obtain the elemental composition.

The BET surface areas of the catalysts were measured by using  $\text{N}_2$  physisorption at 77 K with a Micromeritics TriStar II 3020 apparatus. Before measurements, the samples were dried under vacuum at 298 K for 12 h.

The powder XRD patterns were recorded with a Bruker D8 diffractometer with a  $\text{CuK}\alpha$  radiation source operating at 40 kV and 100 mA with a step size of  $2\theta = 0.01^\circ$  over the range  $20\text{--}80^\circ$ . The freshly prepared catalysts were dried under vacuum at RT. The crystallization treatment of the catalysts was performed in a  $\text{N}_2$  atmosphere at different temperatures.

The TEM images and SAED images were obtained with a FEI Tecnai G2 microscope. All samples were first suspended in ethanol by ultrasound, and then one drop of this slurry was deposited on a carbon-coated copper grid for characterization. The metal particle sizes were estimated on the basis of 100 particles.

$\text{H}_2$ -chemisorption and  $\text{H}_2$ -TPD were performed on a TP-5000 instrument equipped with a thermal conductivity detector supplied by Xianquan Co. Ltd. The sample (100 mg) was first flushed with ultrapure Ar (99.999%, Baoding Zhuoda Gas Co. Ltd.) at 473 K for 1 h and then cooled to 303 K and repeatedly pulse injected with 5 vol%  $\text{H}_2/\text{N}_2$  (Baoding Zhuoda Gas Co. Ltd.) until the hydrogen adsorption peaks became stable.  $\text{H}_2$ -chemisorption measurements were calculated by integrating the areas of the hydrogen adsorption peaks. The sample was then flushed with Ar until the integrator baseline was stable, and  $\text{H}_2$ -TPD analysis was then promptly started at a heating rate of  $10 \text{ K min}^{-1}$  in the range of 303–873 K.

The XPS spectra were recorded on a PHI 1600 spectrometer with monochromatic  $\text{MgK}\alpha$  as the excitation source. The catalyst was

mounted on the sample holder, in which the background pressure was lower than  $2.7 \mu\text{Pa}$ . All the binding energy values were corrected by the C 1s peak of contaminant carbon at 284.6 eV.

### Catalyst activity test

The hydrogenation of ethyl benzoate was performed as follows: ethyl benzoate (5.0 g, 33 mmol), ethanol (70 mL), and the catalyst (0.2 g) were successively added into a 100 mL stainless steel autoclave equipped with a mechanical stirrer and an electrical heating system. The autoclave was first flushed 3 times with  $\text{H}_2$ , followed by evacuation, at RT and then pressurized with  $\text{H}_2$  to 5 MPa and heated to 423 K. Hydrogenation was then performed by stirring the reaction mixture vigorously for 5 h. Hydrogenations of other aromatic carboxylic acids and their derivatives were performed under the same reaction conditions in water.

Reaction mixtures were analyzed by using GC on a 30M SE-54 capillary column, and product structures were confirmed by using GC–MS on an Agilent 5975C spectrometer.

### Acknowledgements

We thank Prof. Laurence M. Harwood for his kind assistance in preparing this article. We gratefully acknowledge financial support from the National Natural Science Foundation of China (21376060) and the Natural Science Foundation of Hebei Province (B2011201017).

**Keywords:** amorphous materials · electron-deficient compounds · hydrogenation · palladium · polymers

- [1] a) A. Roucoux, *Top. Organomet. Chem.* **2005**, *16*, 261–279; b) J. Schulz, A. Roucoux, H. Patin, *Chem. Commun.* **1999**, 535–536.
- [2] a) C. Zhao, D. M. Camaioni, J. A. Lercher, *J. Catal.* **2012**, *288*, 92–103; b) H. Z. Liu, T. Jiang, B. X. Han, S. G. Liang, Y. X. Zhou, *Science* **2009**, *326*, 1250–1252; c) Y. Wang, J. Yao, H. R. Li, D. S. Su, M. Antonietti, *J. Am. Chem. Soc.* **2011**, *133*, 2362–2365; d) R. Herbois, S. Noël, B. Léger, L. Bai, A. Roucoux, E. Monflier, A. Ponchel, *Chem. Commun.* **2012**, *48*, 3451–3453.
- [3] a) Z. Q. Guo, L. Hu, H. H. Yu, X. Q. Cao, H. W. Gu, *RSC Adv.* **2012**, *2*, 3477–3480; b) Y. Wang, X. C. Wang, M. Antonietti, *Angew. Chem.* **2012**, *124*, 70–92; *Angew. Chem. Int. Ed.* **2012**, *51*, 68–89; c) P. Zhang, T. B. Wu, T. Jiang, W. T. Wang, H. Z. Liu, H. L. Fan, Z. F. Zhang, B. X. Han, *Green Chem.* **2013**, *15*, 152–159; d) C. Ziebart, R. Jackstell, M. Beller, *ChemCatChem* **2013**, *5*, 3228–3231.
- [4] C. Hubert, E. G. Bilé, A. Denicourt-Nowicki, A. Roucoux, *Green Chem.* **2011**, *13*, 1766–1771.
- [5] K. Taniya, H. Jinno, M. Kishida, Y. Ichihashi, S. Nishiyama, *J. Catal.* **2012**, *288*, 84–91.
- [6] D. J. M. Snelders, N. Yan, W. J. Gan, G. Laurenczy, P. J. Dyson, *ACS Catal.* **2012**, *2*, 201–207.
- [7] M. A. Keane, *J. Catal.* **1997**, *166*, 347–355.
- [8] a) A. M. Alexander, J. S. J. Hargreaves, *Chem. Soc. Rev.* **2010**, *39*, 4388–4401; b) X. F. Zhang, Q. M. Zhang, A. Q. Zhao, J. Guan, D. M. He, H. Q. Hu, C. H. Liang, *Energy Fuels* **2010**, *24*, 3796–3803; c) G. W. Xie, Z. G. Lv, G. X. Wang, *Mater. Chem. Phys.* **2009**, *118*, 281–283; d) Z. H. Zhu, J. Q. Ma, L. Xu, L. Xu, H. X. Li, H. Li, *ACS Catal.* **2012**, *2*, 2119–2125; e) M. Mo, L. Han, J. G. Lv, Y. Zhu, L. M. Peng, X. F. Guo, W. P. Ding, *Chem. Commun.* **2010**, *46*, 2268–2270.
- [9] a) H. X. Li, S. Y. Zhang, H. S. Luo, *Mater. Lett.* **2004**, *58*, 2741–2746; b) J. H. Shen, Y. W. Chen, *J. Mol. Catal. A-Chem.* **2007**, *273*, 265–276.
- [10] J. W. Park, E. H. Chae, S. H. Kim, J. H. Lee, J. W. Kim, S. M. Yoon, J. Y. Choi, *Mater. Chem. Phys.* **2006**, *97*, 371–378.

- [11] B. J. Liaw, S. J. Chiang, S. W. Chen, Y. Z. Chen, *Appl. Catal. A* **2008**, *346*, 179–188.
- [12] K. S. Suslick, S. B. Choe, A. A. Cichowlas, M. W. Grinstaff, *Nature* **1991**, *353*, 414–416.
- [13] Y. W. Chen, N. Sasirekha, *Ind. Eng. Chem. Res.* **2009**, *48*, 6248–6255.
- [14] W. Y. Wang, Y. Q. Yang, H. A. Luo, H. Z. Peng, F. Wang, *Ind. Eng. Chem. Res.* **2011**, *50*, 10936–10942.
- [15] a) G. Y. Bai, Z. Zhao, L. B. Niu, H. X. Dong, M. D. Qiu, F. Li, Q. Z. Chen, G. F. Chen, *Catal. Commun.* **2012**, *23*, 34–38; b) G. Y. Bai, X. Wen, Z. Zhao, F. Li, H. X. Dong, M. D. Qiu, *Ind. Eng. Chem. Res.* **2013**, *52*, 2266–2272.
- [16] a) Z. B. Yu, M. H. Qiao, H. X. Li, J. F. Deng, *Appl. Catal. A* **1997**, *163*, 1–13; b) Z. J. Wu, S. H. Ge, M. H. Zhang, W. Li, S. C. Mu, K. Y. Tao, *J. Phys. Chem. C* **2007**, *111*, 8587–8593.
- [17] F. A. Harraz, S. E. El-Hout, H. M. Killa, I. A. Ibrahim, *J. Catal.* **2012**, *286*, 184–192.
- [18] A. Nowicki, V. L. Boulaire, A. Roucoux, *Adv. Synth. Catal.* **2007**, *349*, 2326–2330.
- [19] A. B. Bindwal, A. H. Bari, P. D. Vaidya, *Chem. Eng. J.* **2012**, *207–208*, 725–733.
- [20] G. Kyriakou, M. B. Boucher, A. D. Jewell, E. A. Lewis, T. J. Lawton, A. E. Baber, H. L. Tierneym, M. Flytzani-Stephanopoulos, E. C. H. Sykes, *Science* **2012**, *335*, 1209–1212.
- [21] J. Zhu, Y. Jia, M. S. Li, M. H. Lu, Ji. J. Zhu, *Ind. Eng. Chem. Res.* **2013**, *52*, 1224–1233.
- [22] H. Li, J. Liu, S. H. Xie, M. H. Qiao, W. L. Dai, H. X. Li, *J. Catal.* **2008**, *259*, 104–110.
- [23] a) J. F. Geng, D. A. Jefferson, B. F. G. Johnson, *Chem. Eur. J.* **2009**, *15*, 1134–1143; b) C. X. Sun, Z. J. Wu, Y. Z. Mao, X. Q. Yin, L. Y. Ma, D. H. Wang, M. H. Zhang, *Catal. Lett.* **2011**, *141*, 792–798.
- [24] Z. Y. Ma, L. X. Zhang, R. Z. Chen, W. H. Xing, N. P. Xu, *Chem. Eng. J.* **2008**, *138*, 517–522.
- [25] J. J. Zou, Z. Q. Xiong, L. Wang, X. W. Zhang, Z. T. Mi, *J. Mol. Catal. A-Chem.* **2007**, *271*, 209–215.
- [26] B. Liu, M. H. Qiao, J. Q. Wang, K. N. Fan, *Chem. Commun.* **2002**, 1236–1237.
- [27] J. Huang, Y. J. Jiang, N. Vegten, M. Hunger, A. Baiker, *J. Catal.* **2011**, *281*, 352–360.
- [28] J. A. Anderson, A. Athawale, F. E. Imrie, F.-M. Mc Kenna, A. Mc Cue, D. Molyneux, K. Power, M. Shand, R. P. K. Wells, *J. Catal.* **2010**, *270*, 9–15.
- [29] J. M. Khurana, S. Chauhan, G. Bansal, *Monatsh. Chem.* **2004**, *135*, 83–87.
- [30] G. Y. Bai, L. B. Niu, M. D. Qiu, F. He, X. X. Fan, H. Y. Dou, X. F. Zhang, *Catal. Commun.* **2010**, *12*, 212–216.
- [31] P. M. Pojer, *Tetrahedron Lett.* **1984**, *25*, 2507–2508.

---

Received: October 10, 2013

Published online on December 27, 2013